Light scattering by horizontally oriented columns

A.V. Burnashov and A.G. Borovoi

V.E. Zuev Institute of Atmospheric Optics,
Siberian Branch of the Russian Academy of Sciences, Tomsk

Received June 19, 2008

The scattering phase functions for different orientations of hexagonal ice columns in the horizontal plane are considered. Tables of the scattered energy distribution over halo as a function of incidence angle and aspect ratio parameter of the crystal form are presented. It is shown that 50–75% of the scattered energy is redistributed among a small number (≤ 7) of halos. The polarization of the scattered light for different polarizations of the incident radiation is considered. The polarization degree of the scattered radiation is shown to be a qualitative indicator of the number of photon trajectories in a crystal, contributing mostly to the given scattering direction.

Introduction

The study of light scattering by ice crystals in cirrus clouds is one of the most urgent problems of atmospheric optics, because cirrus clouds affect appreciably the radiation and heat balance of the Earth's surface.

Presently, only optical characteristics of ice crystals in case of their chaotic orientation in space are thoroughly studied.[1–6] At the same time, cirrus clouds often contain ice crystals, oriented in the near-horizon plane. There is only a small number of publications concerning the light scattering by ice crystals, oriented predominantly or totally in horizontal plane, but they are either illustrative in character[7–12] or their authors confined themselves only to a narrow range of scattering angles.[13]

Typical shapes of ice crystals in cirrus clouds, which are used in model calculations, are hexagonal plates and columns. Earlier, we have already dealt with the scattering matrix for horizontally oriented hexagonal plates.[14,15] This paper is the next step toward the study of scattering matrices in cirrus clouds; i.e., we consider the main qualitative and quantitative characteristics of the scattering matrix for horizontally oriented hexagonal columns.

1. The scattered light intensity

Usually, ice crystals in the atmosphere are chaotically oriented in space, i.e., their rotation angles with respect to three orthogonal coordinate axes are uniformly distributed. Let this case be called the three-dimensional chaotic orientation and denoted through 3D. However, during fall of crystals in air, the aerodynamic forces orient the particles in such a way that the area of their projection onto the horizontal plane is maximal. For instance, the hexagonal ice plates tend to orient themselves in the direction, parallel to horizon. For hexagonal crystals, call the axis, passing through centers of hexagonal faces, the principal axis. Then, the principal axis of plates is directed vertically, but the rotation angle of the plate relative to the principal axis is distributed uniformly. Call such an orientation the one-dimensional (1D) chaotic orientation for horizontally oriented particles.

For hexagonal columns, the principal crystal axis already lies in the horizontal plane and its direction is distributed uniformly with respect to rotation angle around the vertical. Moreover, usually the column is arbitrarily rotated about the principal axis. Such an orientation will be called the two-dimensional (2D) chaotic orientation of horizontally oriented columns. In rarer cases, the ice columns do not rotate around the principal axis, but keep two rectangular faces parallel to horizon. Such one-dimensional orientation distribution (1D) for horizontally oriented columns is also called the Parry orientation after W.E. Parry, who in 1820 observed the halo, caused by such crystal orientation, and explained the origin of these halos.

The above-mentioned types of crystal orientations encompass situations most frequently occurring in the atmosphere. Therefore, in this paper we consider the hexagonal columns with the 2D and Parry orientations. Note that in the atmosphere more rare types of crystal orientations also take place. The next significant type is the Lovitz orientation, when hexagonal prism rotates around two axes: vertical and axis, passing through the middles of two opposite edges, which connect the rectangular faces of the crystal.

The main characteristic of light, scattered by an arbitrary particle, is the extinction cross section. In a given case, we consider the light scattering in the visible wavelength range, where the light absorption by ice is insignificant. In such cases, the extinction cross section coincides with the absorption cross section.

A characteristic feature of the scattered light in the case of Parry orientation of hexagonal-shaped columns is the scattered light localization on a set of lines on the sphere of scattering directions, which are called the halo. Location of the halo lines depends on the incidence angle θ_0, while the light intensity along these lines is determined by the aspect ratio parameter

0235-6880/08/11 804-08 $02.00 © 2008 Institute of Atmospheric Optics

of crystal shape $F = (\text{height}/\text{diameter})$. For certain values of the aspect ratio, some halos may completely disappear.

The scattered light localization along lines on the sphere of scattering directions is a consequence of one-dimensional crystal rotation, when every trajectory of photons, realized inside crystal in the process of light scattering, draws a line on the sphere of scattering directions during crystal rotation. In contrast to the above-considered case of horizontally oriented plates,[14,15] where all halo has reduced to four circles on the sphere of scattering directions, for 1D oriented columns the number and shape of halo lines sharply increase. The consideration of the shape of halo lines and their classification by photon trajectory type is described in detail in Ref. 12.

In our calculations, we confined ourselves to trajectories, contributing most to the scattered radiation. In particular, we disregarded trajectories, the number of collisions along which was equal or greater than seven. An example of thus obtained halos is shown in Fig. 1.

Most of these halos are well known in the literature and have proper names, which are presented in Table 1. Most notable names are given in Fig. 1.

At present, the literature contains almost no quantitative data on the scattered light intensity in halo for horizontally oriented ice crystals. In order to fill this gap, we calculated the integrated contribution of each halo, indicated in Table 1, to the total scattering cross section. These contributions, which were called the weighting coefficients in our previous paper,[14] are presented in Table 2 for 1D oriented columns. It is seen that the most part of the scattered energy (65–75%), irrespective of the aspect ratio parameter and the incidence angle, is distributed among seven halos Q_1–Q_7.

In the case of 2D oriented columns due to the crystal rotation around the principal crystal axis, most lines of the halos are spread on the sphere of the scattering directions. However, certain trajectories give the same halos as in 1D orientation, because the rotation around the principal axis does not alter the scattering direction. These include the parhelic circle (pc) and subhelic arc (sh.a). Certain other trajectories form small bright regions on the sphere of scattering directions (see Figs. 1*c* and *d*).

Names of these halos are denoted in Table 1 through 2D. The weighting coefficients for the main halos are presented in Table 3. It is seen that these halos account for about 50–75% of the scattered energy.

Of interest is the relationship between circumscribed halo and two halos, l.tg.a and u.tg.a. As it is seen from Table 3, the circumscribed halo and halo pair l.tg.a and u.tg.a cannot occur simultaneously for a fixed incidence angle. This fact is explained just as follows. As is seen from Fig. 1*c*, the halos l.tg.a and u.tg.a are shaped as arcs, which at small incidence angles are concave relative to sun, when they are counted off from the sun. Further, as the incidence angle grows, they are transformed into arcs, convex relative to sun. Starting from 45°, these arcs join into a circle, thus forming circumscribed halo. Hence, the circumscribed halo and halo pair l.tg.a and u.tg.a cannot occur simultaneously.

Up to now, the quantitative characteristics of the scattered light in halo were not considered. We calculated them, but, in view of their large volume, they would be better displayed electronically than in printed form in this paper. Therefore, as an illustration, Figure 2 presents distributions of the scattered light intensity only for one aspect ratio parameter and a few incidence angles.

It is interesting to compare the distribution of the scattered intensity between neighboring figures, corresponding to 1D (to the left) and 2D (to the right) crystal orientations for the same incidence angles. As it is seen, certain halos of 1D orientation are substantially smeared and become indistinguishable when going to 2D orientations; whereas other halos change insignificantly.

2. Scattering matrix

In the previous section, we considered the scattered light intensity for totally unpolarized incident light, i.e., the first element of the scattering matrix. In our calculations, we obtained the total scattering matrix, i.e., 16 independent functions, specified on the sphere of scattering directions. As in our previous work,[15] in this paper we consider the reduced scattering matrix **M**, each column of which has a simple physical meaning of Stokes parameters of the scattered radiation for a given polarization of the incident radiation.

For the halos, which are formed only by one photon trajectory in the crystal, it is obvious that, for incident totally polarized light, the scattered light is also totally polarized. Thus, the polarization degree of the scattered light is a criterion of the number of trajectories, making a significant contribution for a given scattering direction. Figure 3 illustrates this conclusion by the example of two halo lines u.sc.p.a and hel.a for Parry orientation of hexagonal column.

Here, each plot presents one column of the scattering matrix, i.e., the intensity and three parameters characterizing the polarization state of the scattered light, which are defined in Ref. 15. In addition, stars in the plots show the fifth function, namely, the polarization degree, which is the simplest criterion of the light polarization. In Figures 3*b*–*d* the halo is u.sc.p.a. As we see, here the polarization degree is equal to unity. This proves that this halo is formed by one photon trajectory. The right-hand side of Fig. 3 presents the scattering matrix for another halo, hel.a, which is likely to be formed by several photon trajectories. It is interesting to note that the polarization degree in these halos turns out insignificant for the incident totally unpolarized light (Figs. 3*a* and *e*).

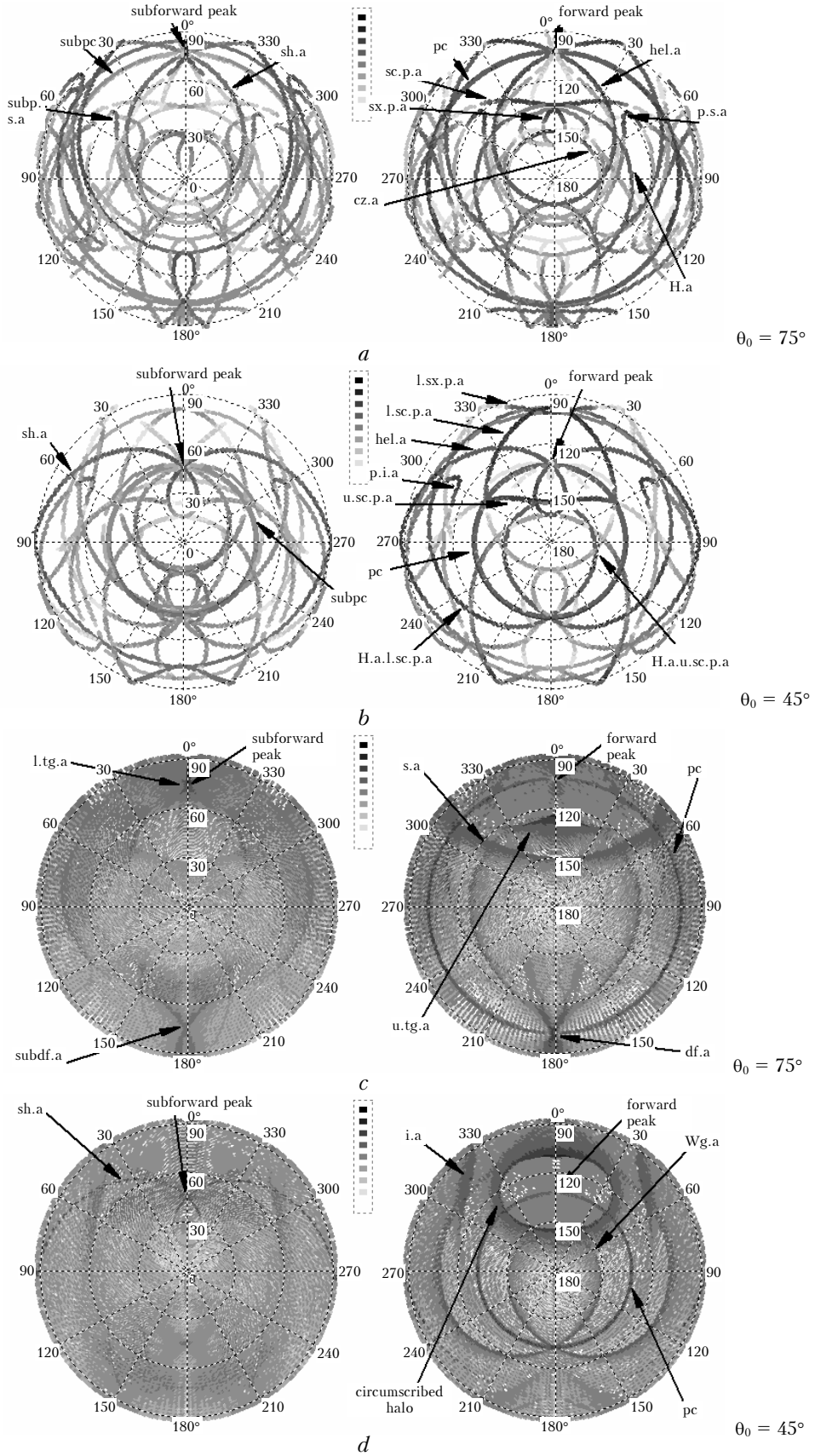

Fig. 1. The halos for 1D (*a*, *b*) and 2D orientations (*c*, *d*) of hexagonal columns at $F = 1.5$; the incidence angle θ_0 is counted off from the zenith direction.

Table 1. Interpreting of the introduced notations of the names of halos for 1D and 2D orientations of hexagonal ice column

Abbreviation	Name
p.i.a	Parry infralateral arc (1D)
l.sc.p.a	Lower suncave Parry arc (1D)
l.sx.p.a	Lower sunvex Parry arc (1D)
u.sc.p.a	Upper suncave Parry arc (1D)
H.a.u.sc.p.a	Hastings arc of upper suncave Parry arc (1D)
H.a.l.sc.p.a	Hastings arc of lower suncave Parry arc (1D)
chor.a	Circumhorizon arc (1D)
subchor.a	Subcircumhorizon arc (1D)
cz.a	Circumzenith arc (1D)
subp.i.a	Parry subinfralateral arc (1D)
p.s.a	Parry supralateral arc (1D)
subp.s.a	Parry subsupralateral arc (1D)
sc.p.a	Suncave Parry arc (1D)
subsc.p.a	Subsuncave Parry arc (1D)
sx.p.a	Sunvex Parry arc (1D)
H.a	Hastings arc (1D)
subu.sc.p.a	Upper subsuncave Parry arc (1D)
pc	Parhelic circle (1D, 2D)
hel.a	Heliac arc (1D, 2D)
sh.a	Subhelic arc (1D, 2D)
subdf.a	Subdiffuse arc (1D, 2D)
df.a	Diffuse arc (1D, 2D)
subpc	Subparhelic circle (1D, 2D)
forward peak	Forward peak (1D, 2D)
subforward peak	Subforward peak (1D, 2D)
Tr.a	Tricker arc (1D, 2D)
Wg.a	Wegener arc (1D, 2D)
s.a	Supralateral arc (2D)
i.a	Infralateral arc (2D)
l.tg.a	Lower tangent arc (2D)
u.tg.a	Upper tangent arc (2D)
circumscribed halo	Circumscribed halo (2D)

Table 2. Distribution of the scattered energy over halo for 1D orientation of hexagonal ice column as a function of aspect ratio *F* and incidence angle θ_0

Weighting coefficient, %	Incidence angle θ_0, deg (counted off from zenith)											
	30			45			60			75		
	F											
	1.5	2.4	4	1.5	2.4	4	1.5	2.4	4	1.5	2.4	4
1	2	3	4	5	6	7	8	9	10	11	12	13
Q_1(hel.a)	5.4	6.1	6.7	7.2	8.4	6.5	14.3	9.8	10.9	18.6	17.3	15.5
Q_2(forward peak)	23.3	26.5	28.3	20.9	26.3	29.9	26.4	31.5	36.7	24.4	26.4	30.9
Q_3(subforward peak)	4.4	3.1	3.6	9.0	5.7	6.2	10.3	11.0	8.1	6.6	8.8	7.0
Q_4(subsc.p.a)	0	0	0	0	0	0	0	0	0	19.9	17.5	14.5
Q_5(l.sc.p.a)	27.7	30.8	33.0	14.0	16.7	18.7	0.1	0.1	0.2	0	0	0
Q_6(l.sx.p.a)	0	0	0	1.8	2.1	2.2	7.1	8.3	9.2	0	0	0
Q_7(u.sc.p.a)	13.5	14.6	15.5	16.7	18.9	20.6	10.5	12.5	14.1	0	0	0
Q_8(cz.a)	0	0	0	0	0	0	0.9	0.6	0.4	1.7	1.2	0.8
Q_9(subp.i.a)	<0.1	<0.1	<0.1	0.5	0.3	0.2	<0.1	<0.1	<0.1	2.0	1.4	0.8
Q_{10}(p.s.a)	0	0	0	0	0	0	0.7	0.3	0.2	2.3	1.6	1.0

Table 2 (continued)

1	2	3	4	5	6	7	8	9	10	11	12	13
Q_{11}(sc.p.a)	0	0	0	0	0	0	0	0	0	3.9	4.9	5.6
Q_{12}(sx.p.a)	0	0	0	0	0	0	0	0	0	1.4	1.6	1.7
Q_{13}(H.a)	0	0	0	0	0	0	2.3	1.6	1.0	1.1	0.8	0.5
Q_{14}(p.i.a)	<0.1	<0.1	<0.1	1.4	0.9	0.6	2.3	1.5	1.0	0	0	0
Q_{15}(H.a.u.sc.p.a)	1.1	0.7	0.5	2.4	1.6	1.0	0	0	0	0	0	0
Q_{16}(H.a.l.sc.p.a)	4.1	2.7	1.7	4.0	2.7	1.7	0	0	0	0	0	0
Q_{17}(subchor.a)	<0.1	0.5	0.3	0	0	0	0	0	0	0	0	0
Q_{18}(subp.s.a)	0	0	0	0	0	<0.1	0.3	<0.1	0	0	0	0
Q_{19}(subu.sc.p.a)	0.1	0.2	0.2	<0.1	<0.1	<0.1	<0.1	<0.1	<0.1	0	0	0
Q_{20}(Tr.a)	0	0	0	0	0	0	<0.1	<0.1	<0.1	<0.1	<0.1	<0.1
Q_{21}(Wg.a)	0	0	0	<0.1	<0.1	<0.1	<0.1	<0.1	<0.1	<0.1	<0.1	<0.1
Q_{22}(pc)	6.2	4.1	2.4	7.4	5.0	3.1	8.6	5.9	3.8	6.5	4.6	3.0
Q_{23}(df.a)	0	0	0	0	0	0	<0.1	<0.1	<0.1	<0.1	<0.1	<0.1
Q_{24}(sh.a)	1.1	0.3	0.1	6.7	3.2	2.2	3.6	5.1	2.9	1.8	1.8	3.6
Q_{25}(subdf.a)	0	0	0	0	0	0	3.1	2.4	1.3	2.1	1.2	0.5
Q_{26}(subpc)	0.7	0.5	<0.1	2.1	1.1	0.4	1.6	1.4	0.9	<0.1	<0.1	<0.1
Q_{27}(chor.a)	5.4	3.7	2.3	0	0	0	0	0	0	0	0	0
Total energy of omitted halos, whose trajectories have ≤ 6 collisions with crystal faces	2.4	2.2	1.4	2.2	2.7	2.3	1.3	1.2	0.9	4.8	3.9	4.7
Total energy of halos, whose trajectories have >7 collisions with crystal faces	4.5	4	4.1	3.8	4.5	6.4	6.6	6.8	8.4	6.5	7.3	9.9

Table 3. Distribution of the scattered energy over halo for 2D orientation of hexagonal ice column as a function of aspect ratio *F* and incidence angle θ_0

Weighting coefficient, %	Incidence angle θ_0, deg (counted off from zenith)											
	30			45			60			75		
	F											
	1.5	2.4	4	1.5	2.4	4	1.5	2.4	4	1.5	2.4	4
forward peak	26.0	28.9	31.0	23.2	29.2	30.3	22.7	28.8	31.3	25.1	27.6	30.2
pc	6.2	4.0	2.5	4.4	2.9	1.9	8.3	5.7	3.7	6.7	4.7	3.1
sh.a	2.9	<1	<1	5.6	2.5	<1	4.6	4.0	1.1	4.0	3.6	2.0
df.a	<1	<1	<1	1.0	<1	<1	1.9	1.7	1.1	1.7	1.3	0.9
l.tg.a	–	–	–	–	–	–	11.0	13.0	14.6	10.1	12.1	13.7
u.tg.a	–	–	–	–	–	–	11.0	13.0	19.0	9.4	11.2	12.7
Circumscribed halo	35.4	39.3	42.0	28.5	32.9	36.2	–	–	–	–	–	–
Total energy from other trajectories with the number of collisions with crystal faces ≤ 6	21.3	19.7	17.9	29.0	25.9	22.6	28.9	19.4	14.2	30.4	25.1	22.2
Total energy from trajectories which have > 7 collisions with crystal faces	8.2	8.1	6.6	8.4	12	10.8	11.5	14.3	15.1	12.7	14.5	15.3

With regards to 2D oriented crystals, here we deal already not with individual lines, but rather with certain regions, to which the halos of Parry-oriented hexagonal column are smeared out, when it rotates axially. Here, the polarization degree again helps to judge about the number of trajectories contributing to some or another region of the sphere of the scattering directions. Figure 4 shows the polarization degree of the scattered light, whose intensity is presented in Fig. 1*c*.

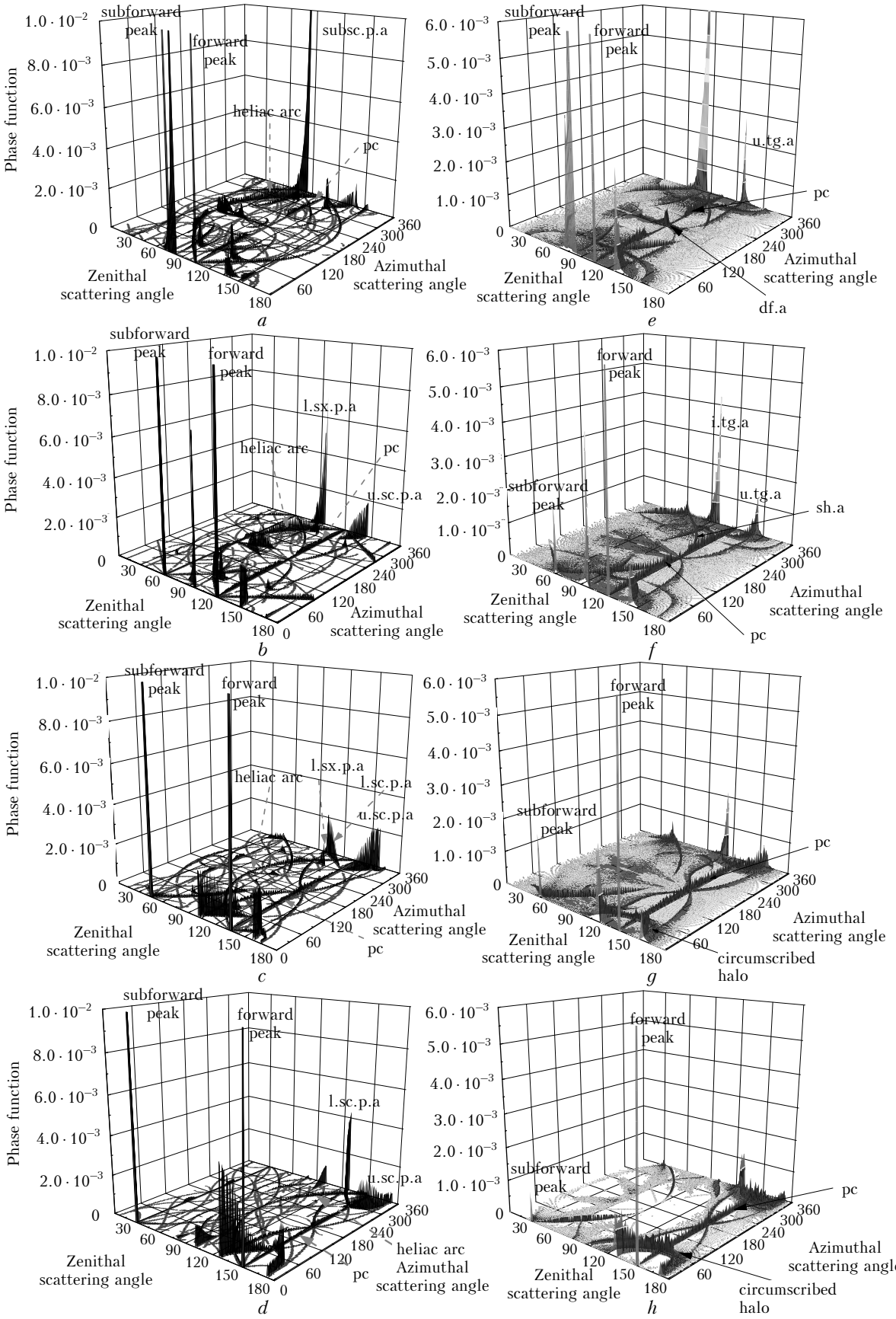

Fig. 2. Distribution of scattered energy over halo: for Parry-oriented hexagonal column (*a*–*d*); for 2D orientation at aspect ratio $F = 1.5$ (*e*–*h*) and incidence angles $\theta_0 = 75$ (*a*, *e*), 60 (*b*, *f*), 45(*c*, *g*), and 30° (*d*, *h*) respectively.

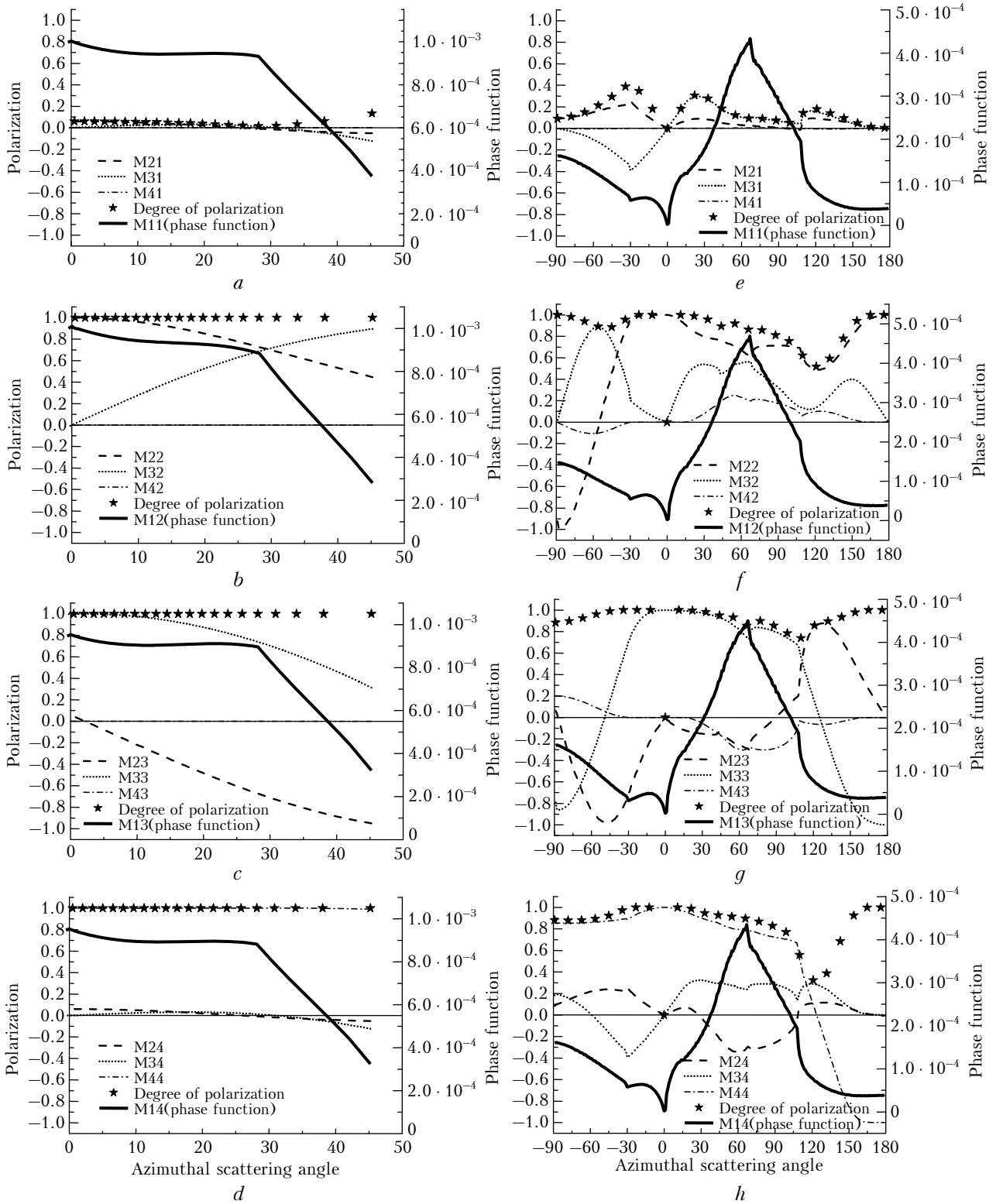

Fig. 3. Scattering matrix for Parry-oriented columns at $F = 1.5$, $\theta_0 = 60°$, u.sc.p.a (*a–d*); hel.a (*e–h*).

Conclusion

The presented calculations of reduced scattering matrix for 1D and 2D orientations suggest that 50–75% of the scattered energy, irrespective of the aspect ratio and the incidence angle, is distributed among seven main halos (Q_1–Q_7, see Table 2) for 1D oriented crystals and among six halos (l.tg.a., u.tg.a., circumscribed halo, forward peak, pc и sh.a, see Table 3) for 2D oriented columns.

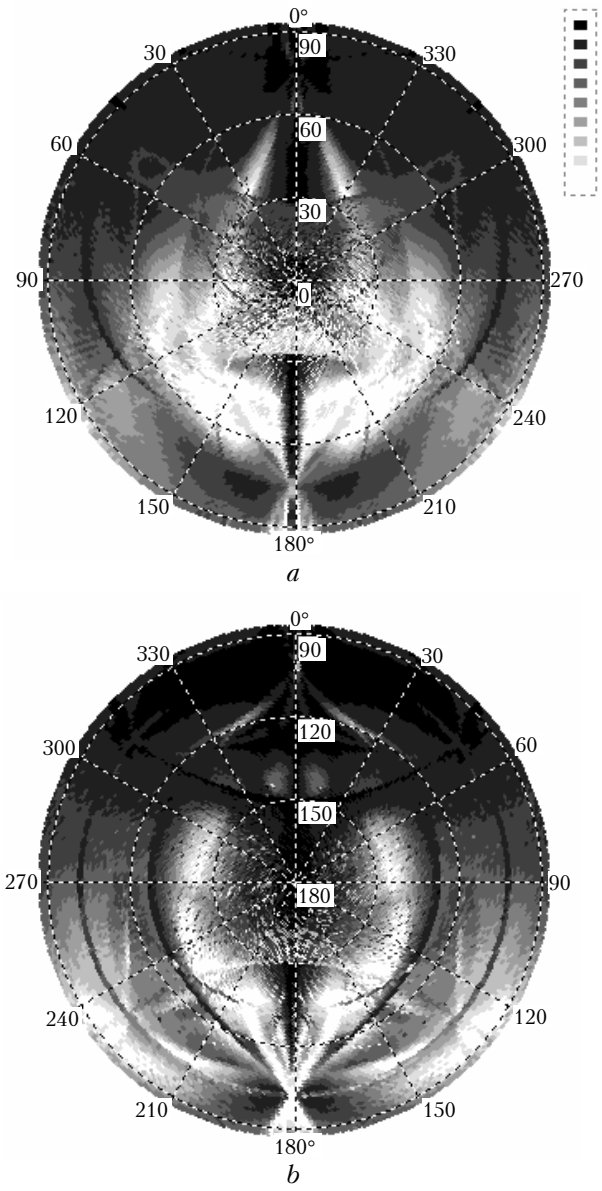

Fig. 4. Second column of the matrix **M** for hexagonal column with 2D orientation and the following parameters: $F = 1.5$, $\theta_0 = 75°$.

In contrast to the case of the horizontally oriented hexagonal plates, considered earlier,[14,15] most marked halos for horizontally oriented columns are formed, as a rule, by one photon trajectory in crystal. Therefore, the polarization degree of the scattered light is often close to unity. The polarization degree can be considered as a criterion for a certain number of trajectories, effectively contributing to a fixed scattering direction.

Acknowledgements

This work is supported by Russian Foundation for Basic Research (Grant No. 06–05–65141) and INTAS (Grant 05-1000008-8024).

References

1. K. Muinonen, K. Lumme, J. Peltoniemi, and W.M. Irwine, Appl. Opt. **28**, No. 15, 3051–3060 (1989).
2. O.A. Volkovitskii, L.N. Pavlova, and A.G. Petrushin, *Optical Properties of Ice Clouds* (Gidrometeoizdat, Leningrad, 1984), 200 pp.
3. A.G. Borovoi and I.A. Grishin, J. Opt. Soc. Am. A **20**, No. 11, 2071–2080 (2003).
4. A.G. Borovoi, N.V. Kustova, and U.G. Oppel, Opt. Eng. **44**, No. 7, 171–208 (2005).
5. P. Yang, and K.N. Liou, in: Kokhanovsky A.A., ed., *Light Scattering Reviews* (Springer-Praxis, Chichester, 2006), pp. 31–71.
6. D.N. Romashov, Atmos. Oceanic Opt. **14**, No. 2, 102–110 (2001).
7. K.-D. Rockwitz, J. Opt. Soc. Am. **28**, No. 19, 4103–4110 (1989).
8. V. Noel, G. Ledanois, H. Chepfer, and P.H. Flamant, Appl. Opt. **40**, No. 24, 4365–4375 (2001).
9. Y. Takano and K.N. Liou, J. Atmos. Sci. **46**, No. 1, 3–19 (1989).
10. Y. Takano and K.N. Liou, Geophys. Res. Lett. **29**, No. 9, 1–4 (2002).
11. W. Tape, *Atmospheric Halos* (American Geophysical Union, Antarctic Research Series, Washington, 1994), V. 64, 139 pp.
12. W. Tape and J. Moilanen, *Atmospheric Halos and the Search the Angle X* (American Geophysical Union, Washington, 2006), 238 pp.
13. D.N. Romashov, B.V. Kaul, and I.V. Samokhvalov, Atmos. Oceanic Opt. **13**, No. 9, 794–800 (2000).
14. A.V. Burnashov and A.G. Borovoi, Atmos. Oceanic Opt. **20**, No. 7, 583–592 (2007).
15. A.V. Burnashov and A.G. Borovoi, Atmos. Oceanic Opt. **20**, No. 11, 880–886 (2007).